した（**図 2**）。次に，過剰量を静脈内投与することで，非晶質ナノシリカの妊娠マウスに対するハザード同定を試みた。その結果，nSP70-N，およびnSP70-C 投与群において異常が認められなかった一方で，nSP70 投与群でのみ，胎仔吸収率の増加とともに，胎仔体重がコントロール群よりも 10% 以上減少するなど，胎仔発育不全を誘発していることが明らかとなった。なお，これら粒子の胎盤への集積や胎仔への移行，および胎仔への影響は，nSP300，および mSP1000 では認められていない。このことから，多くの非晶質ナノシリカ素材が，生殖発生毒性学的視点からも安全であるものの，一部の素材については注意を払う必要があることが示された。以上の検討で見出された nSP70 のハザードは，過剰量における検討ではあるものの，従来型非晶質シリカである nSP300，mSP1000 では認められなかったものであり，一部の非晶質ナノシリカが従来型の非晶質シリカとは異なる生体影響を誘発する可能性を示している。一方で nSP70-N，nSP70-C は，過剰量を静脈内に投与するという実験系にもかかわらず，目立ったハザードは認められなかったことから，これらはきわめて安全性の高い素材であると考えられる。また，これらの知見は逆に，ごく一部の安全性に懸念のあるものに関しても，適切な表面修飾を施すことにより，安全性を担保できる可能性を示している。ナノマテリアルの中にも安全性が高いものとそうでないものがあることはよく知られているが，今後，安全なナノマテリアルを創製するための方法論といったナノ安全科学研究に関する情報をより多く収集することが，ナノマテリアルの安全性評価研究の最重要課題の１つであると考えている。

4. おわりに――ナノ DDS 医薬品の将来像

本総説では，ナノ DDS への適用の現状とともに，最も急がれる安全性確保に関する検討を中心に紹介した。最近では，カーボンナノ素材や非晶質ナノシリカに加え，抗酸化・抗菌活性などを有した白金や

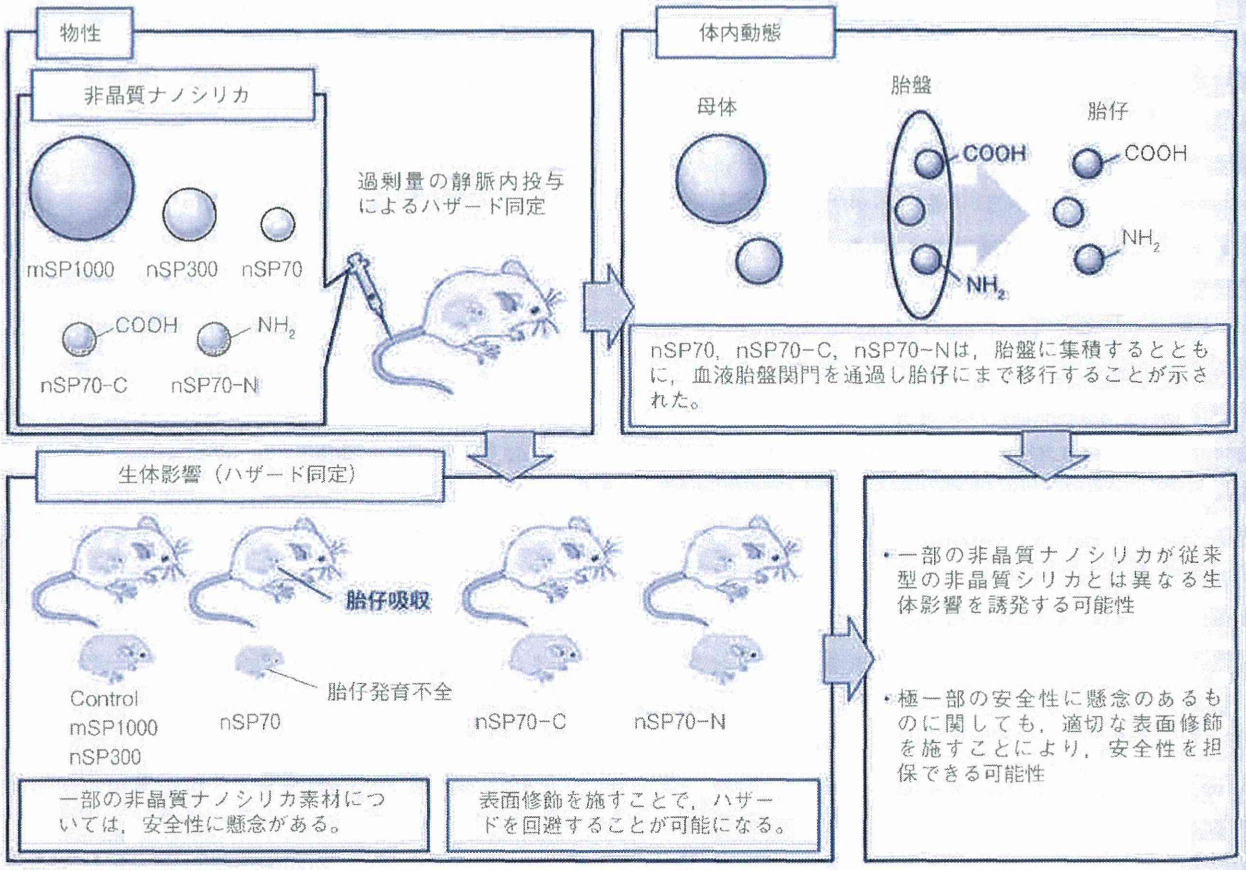

nSP70，nSP70-C，nSP70-N は，胎盤に集積するとともに，血液胎盤関門を通過し胎仔にまで移行することが示された。

一部の非晶質ナノシリカ素材については，安全性に懸念がある。

表面修飾を施すことで，ハザードを回避することが可能になる。

- 一部の非晶質ナノシリカが従来型の非晶質シリカとは異なる生体影響を誘発する可能性
- 極一部の安全性に懸念のあるものに関しても，適切な表面修飾を施すことにより，安全性を担保できる可能性

図 2　生殖発生毒性学的視点からの非晶質ナノシリカの安全性評価

銀などに関して，タンパク質と同等のサブナノサイズ領域（10 nm以下）の素材（サブナノ素材）の開発・実用化も進んでいる。しかし現状では，地球規模でナノマテリアルやサブナノ素材の安全性に警鐘が鳴らされ，OECDを含め，欧米では規制が進んでいるものの，わが国を鑑みると，薬事法・薬局方（医薬品・化粧品・医薬部外品など）をはじめとする各種法律を見ても，ナノマテリアルやサブナノ素材に言及した規制はない。さらに，これら各種法律においては，ナノマテリアルやサブナノ素材を構成する化学物質の構造式（物質名）のみで規制されているため，従前のサブミクロンサイズ（100 nm）以上の素材で安全性が確認されたものや，経験的に安全と考えられるものであれば，ナノ化・サブナノ化されたものでも自由に利用できてしまうことになる。すなわち，①ナノ化・サブナノ化によって，安全性を運命づける『動態特性や効能・効果』が，同一素材であっても，従前のサブミクロンサイズ以上の素材や分子状素材と大きく変動し得ること，②物性などによっても，ナノマテリアルやサブナノ素材に特有の性能が変動し得ること，が理解されつつあるにもかかわらず，品質管理・保障の規制・ガイドライン策定には程遠いのが現状である。したがって，今後は，物性・品質と，動態情報や安全性情報の連関解析を定量的に実施する必要があると考えられる。このように，Nano-Safety Scienceの視点から，ナノマテリアルの安全性情報を収集したうえで，Nano-Safety Designの視点から，安全性の高いものは実用化を推進し，安全性の低いものは表面性状制御をはじめとした適切な方策を講じて安全性を高めていくことで，ヒト健康の確保と同時に，われわれがナノテクノロジーの恩恵を享受しつつナノ産業界の発展も達成できるものと考えている。今後，ナノ開発研究とナノ安全科学研究が強固に連携し，両輪となってともに歩むことで，Sustainable Nanotechnology（いわゆる，持続可能なナノテクノロジー）に資する，地球・環境・ヒトに優しい（安全な）ナノマテリアルの創製，ひいてはナノ医薬品の開発が飛躍的に進歩することを楽しみに，筆者らも一緒にチャレンジしたい。

【引用・参考文献】

1）K. Ajima, et al.：*Mol. Pharm.*, **2**, 475 (2005).
2）Y. Tabata, et al.：*Jpn. J. Cancer Res.*, **88**, 1108 (1997).
3）C. A. Poland, et al.：*Nat. Nanotechnol.*, **3**, 423 (2008).
4）G. Oberdörster, et al.：*J. Nanosci. Nanotechnol.*, **9**, 4996 (2009).
5）H. Nabeshi, et al.：*Part. Fibre Toxicol.*, **8**, 1 (2011).
6）T. Yoshida, et al.：*Nanoscale Res. Lett.*, **6**, 195 (2011).
7）K. Yamashita, et al.：*Inflammation*, **33**, 276 (2010).
8）H. Nabeshi, et al.：*Biomaterials*, **32**, 2713 (2011).
9）K. Yamashita, et al.：*Nat. Nanotechnol.*, **6**, 321 (2011).

〈東阪　和馬／堤　康央〉

Laboratory of Toxicology and Safety Science[1], Graduate School of Pharmaceutical Sciences; Laboratory of Biopharmaceutical Research[2], National Institute of Biomedical Innovation, Osaka, Japan; Cancer Biology Research Center[3], Sanford Research/USD, Sioux Falls, SD, USA; The Center for Advanced Medical Engineering and Informatics[4], Osaka University; Vitamin C60 BioResearch Corporation[5]; Division of Foods[6], National Institute of Health Sciences, Tokyo, Japan

Biochemical and hematologic effects of polyvinylpyrrolidone-wrapped fullerene C_{60} after oral administration

K. Yamashita[1], Y. Yoshioka[1], H. Pan[1], M. Taira[1], T. Ogura[1], T. Nagano[1], M. Aoyama[1], K. Nagano[2], Y. Abe[3], H. Kamada[2,4], S.-I. Tsunoda[2,4], H. Aoshima[5], H. Nabeshi[6], T. Yoshikawa[1], Y. Tsutsumi[1,2,4]

Received July 12, 2012, accepted August 10, 2012

Yasuo Yoshioka, PhD and Yasuo Tsutsumi, Ph.D, Laboratory of Toxicology and Safety Science, Graduate School of Pharmaceutical Sciences, Osaka University, 1-6 Yamadaoka, Suita, Osaka, 565-0871, Japan
yasuo@phs.osaka-u.ac.jp; ytsutsumi@phs.osaka-u.ac.jp

Pharmazie 68: 54–57 (2013) *doi: 10.1691/ph.2013.2708*

The fullerene C_{60} is used in consumer products such as cosmetics owing to its antioxidative effects and is being developed for nanomedical applications. However, knowledge regarding the safety of fullerene C_{60}, especially after oral administration, is sparse. Here, we examined the safety of fullerene C_{60} in mice after 7 d of exposure to orally administered polyvinylpyrrolidone (PVP)-wrapped fullerene C_{60} (PVP-fullerene C_{60}). Mice treated with PVP-fullerene C_{60} showed few changes in the plasma levels of various markers of kidney and liver injury and experienced no significant hematologic effects. Furthermore, the histology of the colon of PVP-fullerene C_{60}-treated mice was indistinguishable from that of control mice. These results suggest that PVP-fullerene C_{60} lacks toxicity after high-dose oral administration and indicate that PVP-fullerene C_{60} can be considered safe for oral medication. These data provide basic information that likely will facilitate the production of safe and effective forms of fullerene C_{60}.

1. Introduction

Advances in nanotechnology have led to the recent development of many nanomaterials, including nanoscale silica particles, titanium dioxide nanoparticles, and carbon nanomaterials (Augustin and Sanguansri 2009; Bowman et al. 2010; Konstantatos and Sargent 2010; Petros and DeSimone 2010). Nanomaterials typically are defined as materials that are 1 to 100 nm in length or diameter. Compared with micro-sized particles, nanomaterials have a high surface area, with increased structural integrity and unique mechanical, chemical, electrical, and magnetic properties. These properties have led to the use of nanomaterials in electronics, foods, and cosmetics and as drug delivery vehicles (Augustin and Sanguansri 2009; Bowman et al. 2010; Konstantatos and Sargent 2010; Petros and DeSimone 2010).

The fullerene C_{60} is one of the most promising nanomaterials because of its unique chemical and physical properties (Chen et al. 2012). Fullerene C_{60} is a remarkably stable compound consisting of 60 carbon atoms, with a diameter of approximately 0.7 nm. Thirty carbon double bonds are present in the structure, to which free radicals easily bond, leading to fullerene C_{60}'s characterization as a "radical sponge" (Krusic et al. 1991). Because of this strong antioxidative feature, fullerene C_{60} is used in cosmetics to reduce oxidative stress in the skin (Benn et al. 2011; Kato et al. 2010). In addition, various water-soluble fullerene C_{60} derivatives have been synthesized for use in a wide range of biologic applications (Aoshima et al. 2009; Kokubo et al. 2008; Lin and Lu 2012; Yin et al. 2009). For example, water-soluble fullerene C_{60} has stronger anti-melanogenic potential than do naturally occurring whitening agents (Kato et al. 2009; Xiao et al. 2007). Furthermore, water-soluble fullerene C_{60} derivatives show promise for the treatment of various inflammatory diseases including rheumatoid arthritis (Hu et al. 2007; Yudoh et al. 2009a,b). Because of these potential biologic applications, several studies have assessed the safety of fullerene C_{60} and its water-soluble derivatives (Aoshima et al. 2010; Kato et al; 2009).

One water-soluble derivative, polyvinylpyrrolidone (PVP)-wrapped fullerene C_{60} (PVP-fullerene C_{60}), is used as a very stable, strongly antioxidative ingredient of cosmetics (Aoshima et al. 2010; Xiao et al. 2007). When applied to the skin, PVP-fullerene C_{60} exhibits protective activity against the apoptosis of keratinocytes that is caused by reactive oxygen species (Xiao et al. 2007). Furthermore, *in vitro* chromosomal aberration assays were conducted using mammalian cells and negative results were reported for PVP-fullerene C_{60} (Aoshima et al. 2010). However, only a few studies have addressed the safety of orally administered PVP-fullerene C_{60} *in vivo*. Therefore assessment of the safety of PVP-fullerene C_{60} after oral administration is a key area in the development of nanomedicines using PVP-fullerene C_{60}.

Here, we examined the safety of PVP-fullerene C_{60} after oral administration to mice. Our data show that oral administration of PVP-fullerene C_{60} induced negligible changes in various biochemical and hematologic parameters. These data provide useful basic safety information that likely will facilitate the development of safe and effective forms of fullerene C_{60}.

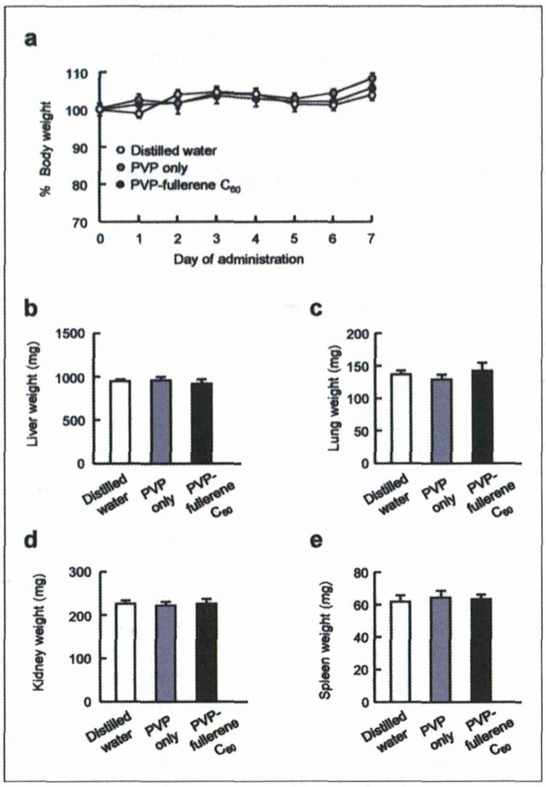

Fig. 1: Effect of oral administration of PVP-fullerene C_{60} on body weight and wet organ weights of mice. PVP-fullerene C_{60} solution in distilled water (50 mg/500 µL/mouse) was administrated orally. Control mice received distilled water or PVP only; all mice were treated by oral gavage daily for 7 d. (a) Body weight during oral administration of PVP-fullerene C_{60}, PVP only, or distilled water. Wet weight of (b) liver, (c) lung, (d) kidney, and (e) spleen after 7 d of treatment. Data are given as mean ± SEM (n = 8)

2. Investigations, results and discussion

We first used dynamic light scattering to measure the hydrodynamic diameters of PVP-fullerene C_{60}. The particle size of PVP-fullerene C_{60} in the distilled water was 127 nm, and its zeta potential was –2.2 mV.

To examine the safety of PVP-fullerene C_{60} after oral administration to mice, each mouse received 0.5 ml of distilled water, PVP only, or PVP-fullerene C_{60} solution by oral gavage once daily for 7 d. Daily behavior including eating, drinking, and activity did not differ between groups; no mice died; and there were no overt differences in body weight gain between groups (Fig. 1a). In addition, wet organ weight after 7 d of oral treatment did not differ significantly between groups (Fig. 1b–e). Hematologic parameters including numbers of red blood cells, platelets, white blood cells, lymphocytes, granulocytes, and monocytes in mice did not show significant differences between groups (Fig. 2a–f). Similarly, plasma biochemical parameters including aspartate aminotransferase (AST) and alanine aminotransferase (ALT) as indicators of hepatic injury and blood urea nitrogen (BUN) as a marker of renal damage did not differ significantly between groups (Fig. 2g–i).

Disease symptom scores and colon length are well-known indicators of colonic inflammation, which is the most common adverse effect after oral administration of test compounds. We scored fecal occult blood as a disease symptom in mice. Similar to those for the distilled water group (1.6 ± 0.1) or PVP only group (1.5 ± 0.1), the score for the PVP-fullerene C_{60}-treated group (1.5 ± 0.1) did not indicate any occult or gross rectal bleeding (Fig. 3a). Furthermore neither colon length (Fig. 3b) nor histology (Fig. 3c–e) differed between groups. Taking together all of our results, we consider that oral administration of 50 mg PVP-fullerene C_{60} daily for 7 d has negligible effects on the health of the colon in mice (Fig. 3).

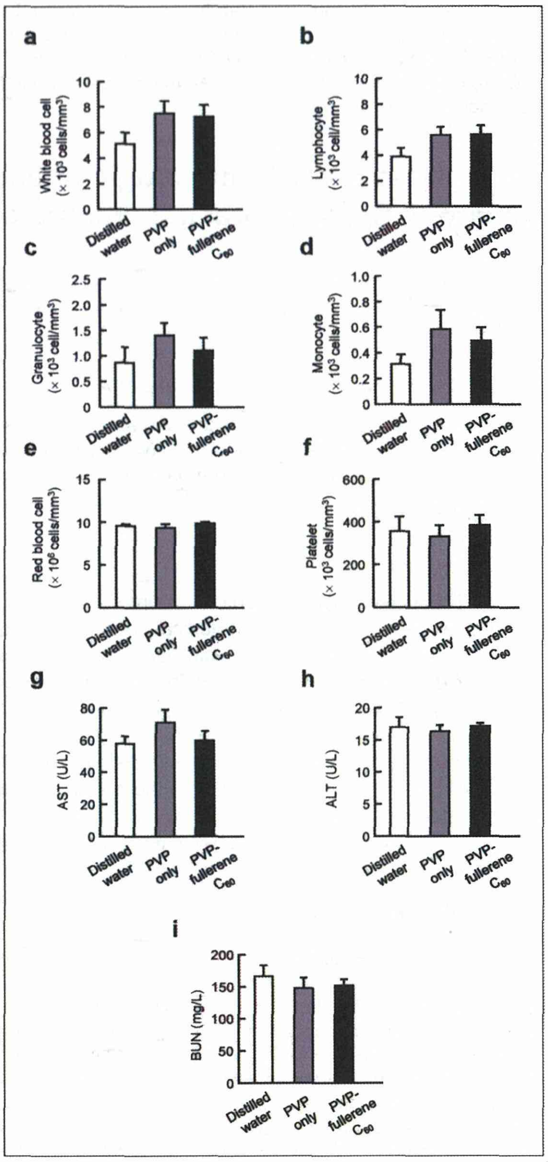

Fig. 2: Effect of oral administration of PVP-fullerene C_{60} on hematologic and biochemical parameters of mice. (a–f) Hematologic parameters were measured after oral administration of PVP-fullerene C_{60} for 7 d. (g–i) Biochemical parameters in the plasma were measured after oral administration of PVP-fullerene C_{60} for 7 d. Data are given as mean ± SEM (n = 6 or 7)

Various *in vitro* and *in vivo* safety assessments of fullerene C_{60} and its derivatives have been reported previously (Metanawin et al. 2011; Nielsen et al. 2008; Zhang et al. 2009). Most studies have shown that fullerene C_{60} and its derivatives are not genotoxic under *in vitro* conditions (Aoshima et al. 2010; Ema

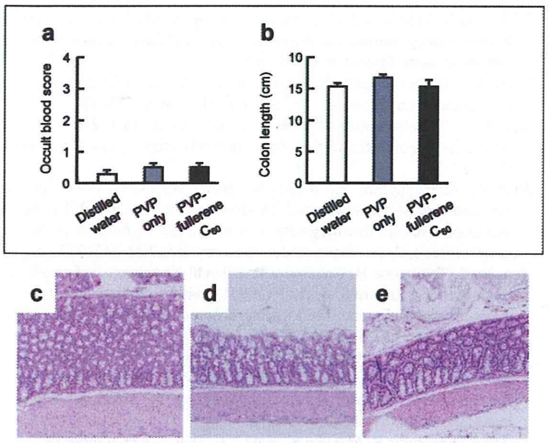

Fig. 3: Effect of oral administration of PVP-fullerene C_{60} on the histology of the colon in mice. (a) Occult blood scores were determined after 7 d of treatment by assessing the consistency, overt blood, and occult blood of feces. (b) Effect of PVP-fullerene C_{60} on colon length. All data are expressed as mean ± SEM (n = 8). Histopathology of the distal colon in C57/BL6 mice after oral administration of distilled water (c), PVP only (d) or PVP-fullerene C_{60} (e) for 7 d. Representative sections were stained with hematoxylin and eosin and examined by using light microscopy

et al. 2012; Shinohara et al. 2009). In addition, water-soluble fullerene C_{60} derivatives can safely be used for dermal and intraperitoneal injection (Aoshima et al. 2010; Gharbi et al. 2005). However, insufficient information is available regarding the safety of water-soluble fullerene C_{60} derivatives after oral administration. In this study, we evaluated the safety and toxicity of oral PVP-fullerene C_{60} by monitoring the body weight, hematologic and biochemical parameters, and colonic health of treated mice. Our results indicate that oral PVP-fullerene C_{60} has no adverse effects on the evaluated parameters in mice.
Guidelines from the Organization for Economic Co-operation and Development (OECD) recommend 28- and 90-d repeated-dose oral toxicity studies in rodents for the safety assessment of chemicals used as nanomaterials. As a first step in the safety assessment of PVP-fullerene C_{60}, we here performed a 7-d oral toxicity study. Now we are trying to perform safety evaluations after long-term exposure.
In conclusion, we showed that oral administration of PVP-fullerene C_{60} induced negligible change in various hematologic, biochemical, and histologic parameters in mice. Although additional studies are needed to further examine the safety of PVP-fullerene C_{60}, we consider that our data provide the basic information that likely will facilitate the development of safe and effective forms of fullerene C_{60}.

3. Experimental

3.1. Particles

PVP-fullerene C_{60} was provided by Vitamin C60 BioResearch (Tokyo, Japan) and is composed of purified fullerene C_{60} and PVP of 60 to 80 kDa. The C_{60} content in PVP-fullerene C_{60} was determined by HPLC analysis on a 5PBB column (Nacalai Tesque, Kyoto, Japan) and found to be approximately 3000 ppm. PVP-fullerene C_{60} was used after 5 min of sonication (280 W output; Ultrasonic Cleaner, AS One, Tokyo, Japan) and 1 min of vortexing. Particle size and zeta potential were measured by using a Zetasizer Nano-ZS (Malvern Instruments, Worcestershire, UK). The mean size and size distribution of particles were measured by using dynamic light scattering; zeta potential was measured by using laser doppler electrophoresis.

3.2. Mice

Female C57BL/6 mice were purchased from Nippon SLC (Kyoto, Japan) and used at 6 weeks of age. Mice were housed in a ventilated animal room maintained at 20 ± 2 °C with a 12:12-h light:dark cycle. Distilled water and sterilized mouse chow were available *ad libitum*. All procedures were performed in accordance with institutional ethical guidelines for animal experiments. During the treatment period, each mouse received 0.5 ml distilled water, PVP only, or PVP-fullerene C_{60} in distilled water (total dose, 50 mg) by oral gavage once daily for 7 d. Mice were euthanized 24 h after administration of the final dose, and liver, lung, kidney, and spleen tissues were harvested and weighed. Blood samples were collected in tubes containing 5 IU/ml heparin sodium, and plasma was harvested. Colons were resected for the determination of colon length (from cecum to anus) and histopathologic examination. Feces were collected and evaluated for occult blood.

3.3. Hematologic analysis

The numbers of white blood cells, granulocytes, lymphocytes, monocytes, red blood cells, and platelets in whole blood were measured by using an auto analyzer (VetScan HMII Hematology System, Abaxis, Union City, CA). Liver function was assessed by measuring plasma levels of AST and ALT. Nephrotoxicity was evaluated by measuring plasma levels of BUN. AST, ALT, and BUN were assayed by using a biochemical autoanalyzer (Fuji Dri-Chem 7000, Fujifilm, Tokyo, Japan).

3.4. Histopathologic examination

For histology of paraffin-fixed tissue, colons were excised and fixed overnight in 10% neutral buffered formalin, embedded in paraffin blocks, sliced, and placed on glass slides. Sections were deparaffinized, rehydrated through a graded series of ethanol, and stained with hematoxylin and eosin. Stained sections were dehydrated through a graded ethanol series and mounted using permount (OCT Compound, Sakura Finetek, Tokyo, Japan). Representative histologic images were recorded by a CCD digital camera that was affixed to a microscope. Fecal occult blood was scored by using the Coloscreen Occult Blood Card Test (Shionogi, Osaka, Japan), with the scale ranging from 0 for negative to 4 for strongly positive.

3.5. Statistical analysis

All results are presented as mean ± standard error of the mean (SEM). Statistical significance in differences was evaluated by analysis of variance (ANOVA) followed by Bonferroni correction. The *P* value used to define significance ($P < 0.05$).

Competing interests: The authors declare that there are no conflicts of interest.

Acknowledgements: This study was supported in part by Grants-in-Aid for Scientific Research from the Ministry of Education, Culture, Sports, Science and Technology of Japan (MEXT), and from the Japan Society for the Promotion of Science (JSPS); and by a the Knowledge Cluster Initiative (MEXT); by Health Labour Sciences Research Grants from the Ministry of Health, Labor and Welfare of Japan (MHLW); by a Global Environment Research Fund from Minister of the Environment; by Food Safety Commission (Cabinet Office); by The Cosmetology Research Foundation; by The Smoking Research Foundation; by The Takeda Science Foundation; by The Nagai Foundation Tokyo; by The Research Foundation for Pharmaceutical Sciences; and by The Japan Food Chemical research Foundation.

References

Aoshima H, Kokubo K, Shirakawa S, Ito M, Yamana S, Oshima T (2009) Antimicrobial activity of fullerenes and their hydroxylated derivatives. Biocontrol Sci 14: 69–72.
Aoshima H, Yamana S, Nakamura S, Mashino T (2010) Biological safety of water-soluble fullerenes evaluated using tests for genotoxicity, phototoxicity, and pro-oxidant activity. J Toxicol Sci 35: 401–409.
Augustin MA, Sanguansri P (2009) Nanostructured materials in the food industry. Adv Food Nutr Res 58: 183–213.
Benn TM, Westerhoff P, Herckes P (2011) Detection of fullerenes (C60 and C70) in commercial cosmetics. Environ Pollut 159: 1334–1342.
Bimbo LM, Sarparanta M, Santos HA, Airaksinen AJ, Makila E, Laaksonen T, Peltonen L, Lehto VP, Hirvonen J, Salonen J (2010) Biocompatibility of thermally hydrocarbonized porous silicon nanoparticles and their biodistribution in rats. ACS Nano 4: 3023–3032.
Bowman DM, van Calster G, Friedrichs S (2010) Nanomaterials and regulation of cosmetics. Nat Nanotechnol 5: 92.
Chen Z, Ma L, Liu Y, Chen C (2012) Applications of functionalized fullerenes in tumor theranostics. Theranostics 2: 238–250.

Ema M, Tanaka J, Kobayashi N, Naya M, Endoh S, Maru J, Hosoi M, Nagai M, Nakajima M, Hayashi M, Nakanishi J (2012) Genotoxicity evaluation of fullerene C60 nanoparticles in a comet assay using lung cells of intratracheally instilled rats. Regul Toxicol Pharmacol 62: 419–424.

Gharbi N, Pressac M, Hadchouel M, Szwarc H, Wilson SR, Moussa F (2005) [60]fullerene is a powerful antioxidant in vivo with no acute or subacute toxicity. Nano Lett 5: 2578–2585.

Hu Z, Liu S, Wei Y, Tong E, Cao F, Guan W (2007) Synthesis of glutathione C60 derivative and its protective effect on hydrogen peroxide-induced apoptosis in rat pheochromocytoma cells. Neurosci Lett 429: 81–86.

Kato S, Aoshima H, Saitoh Y, Miwa N (2009) Biological safety of Lipo-Fullerene composed of squalane and fullerene-C60 upon mutagenesis, photocytotoxicity, and permeability into the human skin tissue. Basic Clin Pharmacol Toxicol 104: 483–487.

Kato S, Taira H, Aoshima H, Saitoh Y, Miwa N (2010) Clinical evaluation of fullerene-C60 dissolved in squalane for anti-wrinkle cosmetics. J Nanosci Nanotechnol 10: 6769–6774.

Kokubo K, Tochika S, Kato M, Sol Y, Oshima T (2008) AlCl3-catalyzed tandem acetylation of hydroarylated [60]fullerenes. Org Lett 10: 3335–3338.

Konstantatos G, Sargent EH (2010) Nanostructured materials for photon detection. Nat Nanotechnol 5: 391–400.

Krusic PJ, Wasserman E, Keizer PN, Morton JR, Preston KF (1991) Radical reactions of c60. Science 254: 1183–1185.

Lin CM, Lu TY (2012) C60 Fullerene Derivatized Nanoparticles and their Application to Therapeutics. Recent Pat Nanotechnol 6: 105–113.

Metanawin T, Tang T, Chen R, Vernon D, Wang X (2011) Cytotoxicity and photocytotoxicity of structure-defined water-soluble C60/micelle supramolecular nanoparticles. Nanotechnology 22: 235604.

Nielsen GD, Roursgaard M, Jensen KA, Poulsen SS, Larsen ST (2008) In vivo biology and toxicology of fullerenes and their derivatives. Basic Clin Pharmacol Toxicol 103: 197–208.

Petros RA, DeSimone JM (2010) Strategies in the design of nanoparticles for therapeutic applications. Nat Rev Drug Discov 9: 615–627.

Shinohara N, Matsumoto K, Endoh S, Maru J, Nakanishi J (2009) In vitro and in vivo genotoxicity tests on fullerene C60 nanoparticles. Toxicol Lett 191: 289–296.

Xiao L, Matsubayashi K, Miwa N (2007) Inhibitory effect of the water-soluble polymer-wrapped derivative of fullerene on UVA-induced melanogenesis via downregulation of tyrosinase expression in human melanocytes and skin tissues. Arch Dermatol Res 299: 245–257.

Yamago S, Tokuyama H, Nakamura E, Kikuchi K, Kananishi S, Sueki K, Nakahara H, Enomoto S, Ambe F (1995) In vivo biological behavior of a water-miscible fullerene: 14C labeling, absorption, distribution, excretion and acute toxicity. Chem Biol 2: 385–389.

Yin JJ, Lao F, Fu PP, Wamer WG, Zhao Y, Wang PC, Qiu Y, Sun B, Xing G, Dong J, Liang XJ, Chen C (2009) The scavenging of reactive oxygen species and the potential for cell protection by functionalized fullerene materials. Biomaterials 30: 611–621.

Yudoh K, Karasawa R, Masuko K, Kato T (2009a) Water-soluble fullerene (C60) inhibits the development of arthritis in the rat model of arthritis. Int J Nanomedicine 4: 217–225.

Yudoh K, Karasawa R, Masuko K, Kato T (2009b) Water-soluble fullerene (C60) inhibits the osteoclast differentiation and bone destruction in arthritis. Int J Nanomedicine 4: 233–239.

Zhang LW, Yang J, Barron AR, Monteiro-Riviere NA (2009) Endocytic mechanisms and toxicity of a functionalized fullerene in human cells. Toxicol Lett 191: 149–157.

Nanoscale

RSC Publishing

PAPER

Cite this: *Nanoscale*, 2013, **5**, 2317

Synthesis of a new class of fullerene derivative $Li^+@C_{60}O^-(OH)_7$ as a "cation-encapsulated anion nanoparticle"†

Hiroshi Ueno,[a] Ken Kokubo,*[a] Eunsang Kwon,[b] Yuji Nakamura,[a] Naohiko Ikuma[a] and Takumi Oshima[a]

Received 12th November 2012
Accepted 3rd January 2013

DOI: 10.1039/c3nr33608e

www.rsc.org/nanoscale

Metal encapsulation into a cage and chemical modification on the outer surface of fullerenes endow them with some unique characteristic properties. Although the derivatization of endohedral fullerenes holds promise for producing novel new nano-carbon materials, there are few reports about such compounds. Herein, we report the synthesis of lithium encapsulated fullerenol $Li^+@C_{60}O^-(OH)_7$ using a fuming sulfuric acid method from $[Li^+@C_{60}](PF_6^-)$ and characterization of its structure by IR, NMR, FAB mass spectroscopy, and elemental analysis. The hydroxylation of $[Li^+@C_{60}](PF_6^-)$ is site-selective to preferentially give a single isomer (ca. 70%) with two minor isomers in marked contrast to the reaction of empty C_{60}. We conclude from the analysis of radical species produced in the reaction of a C_{60} cage with fuming sulfuric acid that this unusual site-selective hydroxylation is caused by the lower HOMO level of $Li^+@C_{60}$ than that of empty C_{60}. Furthermore, our results clearly indicate that the internal lithium cation is interacted with the introduced hydroxyl groups, and thus the properties of endohedral fullerenes can be controlled by the external modification of a fullerene cage.

Introduction

Since the first report of macroscopic synthesis, complete isolation, and structural determination of lithium encapsulated fullerene $[Li^+@C_{60}](SbCl_6^-)$,[1] it has attracted growing attention owing to the strong electron accepting ability as well as the semiconducting property in the fields of organic electronics and materials chemistry.[2] However, details on the chemical modification of a fullerene cage and on the properties of resulting derivatives have not been well investigated except for the recent successful synthesis of $[Li^+@PCBM](PF_6^-)$.[3] Such external functionalization of endohedral metallofullerenes, especially solubilization in polar solvents, can be a versatile and promising protocol for controlling the physicochemical properties and the static behavior of encapsulated metal ions in a π-conjugated molecular cage.

On the other hand, polyhydroxylated fullerene, so-called fullerenol $C_{60}(OH)_n$, has been one of the most intriguing fullerene-based materials due to the prominent hydrophilicity and bioactivities with relatively low toxicity.[4–8] Various types of synthetic procedures for variously hydroxylated fullerenols[9–13] have been reported so far including our highly hydroxylated $C_{60}(OH)_{36}$ and $C_{60}(OH)_{44}$.[14,15] As expected, these fullerenols consist of a mixture of a wide variety of isomers with various numbers and positions of introduced hydroxyl groups, and only an average number of hydroxyl groups can be determined by elemental analysis except for recently synthesized $C_{60}(OH)_8$ as a single isomer.[16]

Considering these situations, it is no doubt that metal encapsulated fullerenols will play a significant role as a new class of functionalized nanomaterials not only in life science but also in materials chemistry. However, only a few cases are known; *e.g.*, Gd-encapsulated fullerene[17,18] and our previously reported mixture of Li-encapsulated and empty fullerenols prepared from the $Li@C_{60}$ cluster with an encapsulation ratio of only 12%.[19]

Herein, we report the unusual site-selective synthesis of Li-encapsulated fullerenol $Li^+@C_{60}O^-(OH)_7$ as a single major isomer along with two minor isomers when pure $[Li^+@C_{60}](PF_6^-)$ was treated with fuming sulfuric acid. Although the regiochemical positions of hydroxyl groups could not be determined due to its C_1 symmetrical structure, its unique physicochemical properties based on both the internal Li^+ and the external –OH groups as well as the mechanistic aspects on site-selective hydroxylation were revealed.

Results and discussion

The hydroxylation of $[Li^+@C_{60}](PF_6^-)$ was carried out using the reported procedures under the optimized reaction conditions

---

[a] *Division of Applied Chemistry, Graduate School of Engineering, Osaka University, 2-1 Yamadaoka, Suita, Osaka 565-0871, Japan. E-mail: kokubo@chem.eng.osaka-u.ac.jp; Fax: +81-6-6879-4593; Tel: +81-6-6879-4592*

[b] *A Research and Analytical Center for Giant Molecules, Graduate School of Science, Tohoku University, 6-3 Aza-aoba, Aramaki, Aoba-ku, Sendai, Miyagi 980-8578, Japan*

† Electronic supplementary information (ESI) available: Experimental details, HPLC chart, ^{13}C NMR, FAB MS, UV-vis, ^{31}P and ^{19}F NMR, and Vis-NIR spectra of compounds. See DOI: 10.1039/c3nr33608e

(Scheme 1). The product was characterized through infrared spectroscopy (IR), nuclear magnetic resonance spectroscopy (NMR), fast atom bombardment mass spectroscopy (FAB MS), thermogravimetric analysis (TGA) as well as the elemental analysis. The IR spectrum of the product is shown in Fig. 1 along with that of the empty fullerenol $C_{60}(OH)_n$ ($n = 10$, as the average structure of a mixture of isomers) synthesized independently by the same fuming sulfuric acid method as a reference. The spectrum showed five characteristic bands at 3281, 1625, 1418, 1081 and 1040 cm^{-1} assignable to νO–H, νC=C, δ_sC–O–H and two types of νC–O, respectively. These absorption peaks clearly confirm the formation of a fullerenol cage. Of interest is that the splitting of the νC–O peak was observed only for Li^+ encapsulated fullerenol. The higher energy band at 1080 cm^{-1} (by *ca.* 40 cm^{-1}) implies the appearance of the fullerenoxide $C–O^-$ bond with enhanced bond order probably because of the deprotonation from one of the OH groups by electrostatic repulsion against the encapsulated Li^+ ion.[20]

The encapsulated lithium cations were clearly detected by ^{7}Li NMR spectroscopy. In the spectrum obtained in DMSO-d_6, three characteristic signals were observed in the range of −15 to −19 ppm relative to LiCl in D_2O as an external standard (Fig. 2a). The observed upfield chemical shifts apparently suggest the encapsulation of Li^+ by the π-conjugated fullerene cage. The abnormal higher upfield shift of the product than that of $[Li^+@C_{60}](SbCl_6^-)$ salt (−10.5 ppm)[1] may be caused by the increased diamagnetic shielding effect of the appeared surface negative charge interacting with the inner lithium cation as already reported in our recent paper.[19] These three sharp signals seem to correspond to a major isomer (−16.7 ppm, *ca.* 70%) and two minor isomers (−15.3 and −18.2 ppm, *ca.* 10 and 20% by integration ratio), respectively. This ^{7}Li NMR spectrum is quite different from the highly broadened previous one,[19] implying the formation of the less number of isomers possibly due to the unusual site-selective hydroxylation. Surprisingly, as shown in Fig. 2b, seven tall sharp peaks (*a–g*) along with four smaller minor peaks (*) assignable to –OH groups were clearly detected by ^{1}H NMR spectroscopy, whereas the empty fullerenol synthesized from pristine C_{60} showed a highly broadened signal centred at 7 ppm on account of the presence of a wide variety of isomers. These sharp peaks were found to disappear by addition of D_2O due to H–D exchange of the hydroxyl protons. The product distribution of isomers was also confirmed by HPLC analysis, consistent with ^{7}Li NMR (Fig. S1†). Whereas the three isomers could be detected clearly, their preparative separation was failed because (1) we could not secure enough amount of starting lithium encapsulated fullerene and (2) the product easily degraded during the separation process.

It was also noted that the ^{13}C NMR spectrum provided several signals assigned for sp^3 C–OH carbons at 72–77 ppm, probably eight large peaks and four small peaks, together with

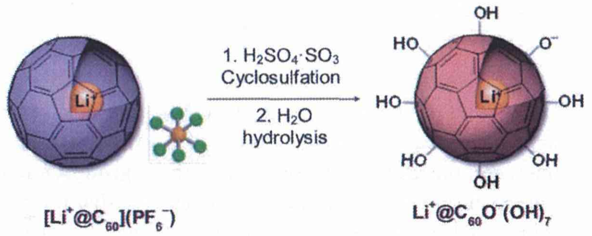

Scheme 1 Synthesis of lithium encapsulated fullerenol.

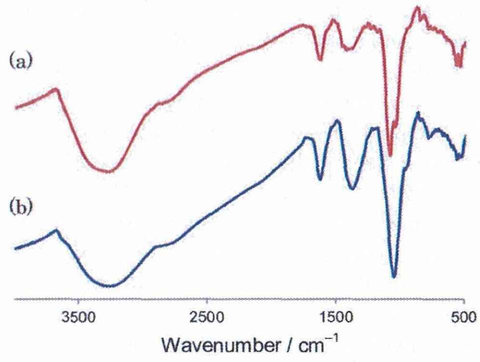

Compound	Absorptions / cm^{-1} (assigned to)			
Product	3281 (νO–H)	1625 (νC=C)	1418 (δ_sC–O–H)	1081, 1040 (νC–O)
$C_{60}(OH)_{10}$	3250	1622	1373	1044

Fig. 1 IR spectra and the typical absorptions (cm^{-1}) of (a) the Li^+ encapsulated fullerenol and (b) reference empty fullerenol $C_{60}(OH)_{10}$.

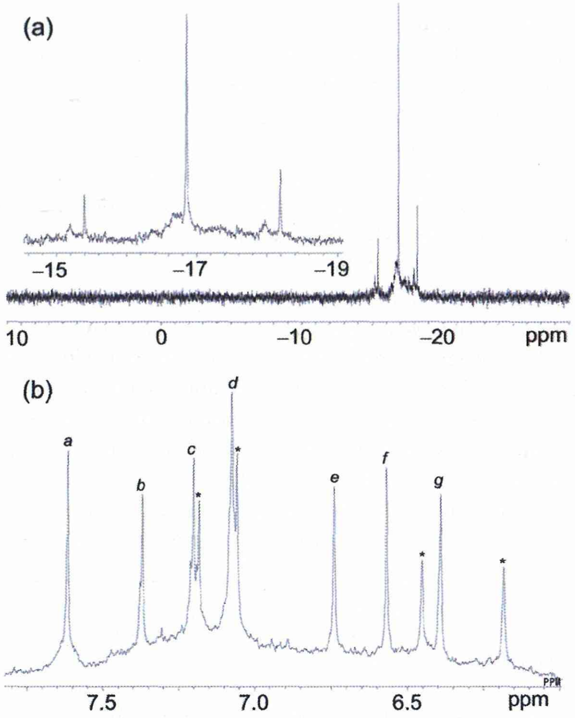

Fig. 2 (a) ^{7}Li NMR spectrum and (b) ^{1}H NMR spectrum of the Li^+-encapsulated fullerenol in DMSO-d_6. The D_2O solution of LiCl was used as an external standard for the measurement of ^{7}Li NMR.

over 40 signals of sp^2 carbons at 140–160 ppm (Fig. S2†), in conformity with the C_1 symmetrical structure. Unfortunately, however, the peaks corresponding to the minor isomers could not be clearly observed due to the small amount of the sample even on 60 000 times accumulation.

Furthermore, we also confirmed the formation of lithium encapsulated fullerenol by positive mode fast atom bombardment mass spectroscopy (FAB MS) (Fig. 3, and the details are shown in Fig. S3†) and UV-vis-NIR spectroscopy (Fig. S4†). The peak at $m/z = 863$ was attributed to Li$^+$@C$_{60}$O$^-$(OH)$_7$, suggesting the encapsulation of the lithium cation. The high resolution matrix-assisted laser desorption ionisation time of flight (MALDI-TOF) mass spectroscopy also showed the molecular ion peak assignable to the same species. The UV-vis-NIR spectrum of the product was essentially the same as that of the empty one. Finally, the structure was deduced from the elemental analysis as being almost the same as the formula of Li$^+$@C$_{60}$-O$^-$(OH)$_7$·4H$_2$O (Table 1).

These findings strongly indicate that the Li$^+$ encapsulated fullerenols consist of a single major regioisomer (*ca.* 70%) of Li$^+$@C$_{60}$O$^-$(OH)$_7$ which has seven OH groups and one fullerenoxide (C$_{60}$O$^-$) moiety with C_1 symmetry. Similar to the minor products it may be conceived of having a pair of (1) different regioisomers of the major one or (2) the more or less hydroxylated fullerenols.

Very interestingly, we confirmed that the counter anion PF$_6^-$ was completely lost in the product on the basis of ^{31}P and ^{19}F NMR spectroscopy (Fig. S5 and S6†). This phenomenon can be explained by the formation of a fullerenoxide (C$_{60}$O$^-$) anion moiety which no longer needs the counter anion such as PF$_6^-$ (*vide supra*). The negative charge of fullerenoxide (C$_{60}$O$^-$) may be partly dispersed on the highly conjugated fullerene surface on account of the favourable electrostatic interaction with inner Li$^+$ ions. As a result, the Li$^+$ would highly be inclined toward one side of the inner wall of C$_{60}$ as similarly reported for [Li$^+$@C$_{60}$](SbCl$_6^-$) (ref. 1) and [Li$^+$@PCBM](PF$_6^-$).[3] We have confirmed such Li$^+$ behavior by DFT calculation as previously reported.[19] Therefore, we propose the structure of Li$^+$@C$_{60}$-O$^-$(OH)$_7$ without any free counter anion, and thus the compound could be considered as a "cation encapsulated anion nanoparticle".

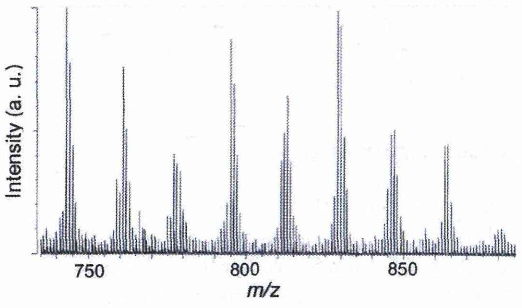

Fig. 3 Positive mode FAB mass spectrum of the product. The peak observed at $m/z = 863$ attributed to Li$^+$@C$_{60}$O$^-$(OH)$_7$ (M + H$^+$) was detected. The other peaks at 743, 761, 777, 795, 811, 829, and 845 were fragment signals assignable to LiC$_{60}$O(OH)$_{0-6}$, respectively.

Table 1 Elemental analysis of the product

Average structure	Elemental analysis^a (%)	Water content^{a,b} (wt%)
Product	C: 77.16, H: 1.84	5.1
Li@C$_{60}$O(OH)$_7$·4H$_2$O	(C: 77.10, H: 1.62)	(7.7)

^{a} Values in parentheses are calculated data. ^{b} Water content was determined by TGA.

Why did the hydroxylation reaction of lithium encapsulated fullerene take place site-selectively? The time course of Vis-NIR spectra of the reaction intermediate in the cyclosulfation step[9] recorded in fuming sulfuric acid H$_2$SO$_4$·SO$_3$ at room temperature provided telling clues about the reason. The spectrum just after the reaction started is shown in Fig. 4 together with the case of empty C$_{60}$ under the same conditions. The broad peak around 823 nm (blue line) in the reaction of empty fullerene with fuming sulfuric acid suggests the generation of divalent cations of C$_{60}$ (C$_{60}^{2+}$) through the two-electron oxidation which was induced by strong acceptor H$_2$S$_2$O$_7$ resulting from SO$_3$.[21–23] By contrast, the characteristic band of the Vis-NIR spectrum at 964 nm (red line) and the ESR spectrum recorded in fuming sulfuric acid (Fig. 5) for Li$^+$ encapsulated one indicated that the cation radical (Li$^+$@C$_{60}^{\cdot+}$) was exclusively produced through one-electron oxidation.[24] The lower g value (2.0016) compared

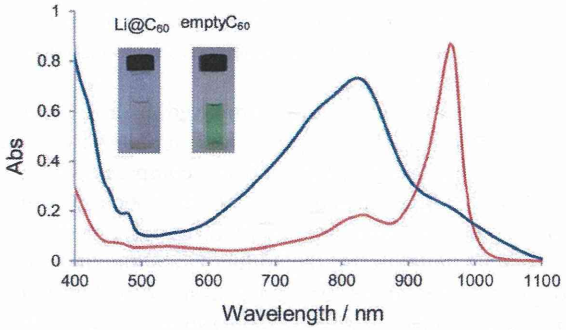

Fig. 4 Vis-NIR spectra of the reaction intermediate during the cyclosulfation of [Li$^+$@C$_{60}$](PF$_6^-$) (red) and empty fullerene (blue) in fuming sulfuric acid. Inset: the visual color of the solutions.

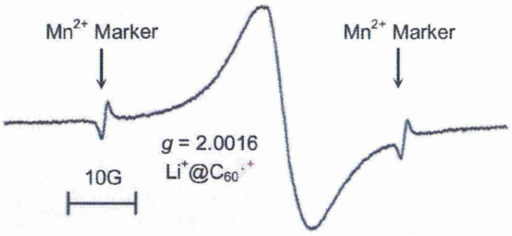

Fig. 5 ESR spectrum of the reaction intermediate during the cyclosulfation of [Li$^+$@C$_{60}$](PF$_6^-$) recorded in fuming sulfuric acid at 298 K calibrated by using a Mn^{2+} marker.

with the reported empty C_{60} radical cation and the line broadening was probably due to the polarity of fuming sulfuric acid and internal lithium cation.[25–27]

These differences in the ionization potential between the Li^+ encapsulated C_{60} and the empty one can be rationalized by comparing their UV-vis spectra as well as reduction potentials. The UV-vis spectra of these fullerenes are almost superimposable, because of essentially the same HOMO–LUMO energy gaps. However, the first reduction potential, which corresponds to LUMO, of Li^+ encapsulated C_{60} was found to be 0.7 V more reducible than the empty one on cyclic voltammetry (CV) measurement.[1] Therefore, the first oxidation potential which corresponds to the HOMO should also be different by *ca.* 0.7 V due to the strong electron accepting ability of Li^+ and thus monovalent $Li^+@C_{60}{}^{+\cdot}$ seems to be sluggishly formed on fuming sulfuric acid oxidation, while the empty C_{60} can be easily oxidized to the divalent cation species.[21–23] Indeed, monovalent cation radical $Li^+@C_{60}{}^{+\cdot}$ was found to be persistent several days in fuming sulfuric acid, whereas the divalent one degraded within several hours. Therefore, the cyclosulfation reaction of $[Li^+@C_{60}](PF_6{}^-)$ was quite slow as compared with the reaction of the empty one (see Fig. S7–S9†). This difference in the stability (*i.e.*, reactivity) of the oxidized species is partly responsible for the difference in the site-selectivity of the multi-step addition of fuming sulfuric acid.[28–30] The Vis-NIR spectrum of the reaction intermediate of the "$Li@C_{60}$ cluster"[19] in fuming sulfuric acid was also recorded for comparison (Fig. S10†). However, no clear peak at ~960 nm which can be seen in the case of $[Li^+@C_{60}](PF_6{}^-)$ was observed probably due to the heterogeneous cluster nature of $Li^+@C_{60}{}^{-\cdot}$ surrounded by neutral C_{60} molecules. This electronic difference as well as the steric restriction could result in the unselective hydroxylation of the $Li@C_{60}$ cluster.[19]

One of the effects of the introduced hydroxyl groups to $[Li^+@C_{60}](PF_6{}^-)$ was the improvement of solubility. Although the solubility of $[Li^+@C_{60}](PF_6{}^-)$ is low compared with pristine C_{60}, $Li^+@C_{60}O^-(OH)_7$ could be dissolved in polar solvents such as DMSO and DMF comparable with the empty one. Indeed, the particle size analysis by the induced grating (IG) method[31] showed the small and narrow particle size distribution (*ca.* 1.1 nm, original molecular size) in DMSO solution (Fig. 6). The size was also confirmed by scanning prove microscopy (SPM) for the sample prepared by applying the highly diluted aqueous solution of fullerenol to a mica plate and drying it (Fig. 6).

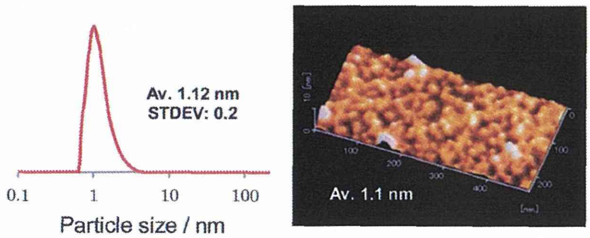

Fig. 6 Particle size distribution of $Li^+@C_{60}O^-(OH)_7$ in DMSO solution (1 mM) measured by the IG method (left) and SPM particle size analysis for $Li^+@C_{60}O^-(OH)_7$ on a mica plate (right).

Conclusions

In summary, we synthesized $Li^+@C_{60}O^-(OH)_7$ using a fuming sulfuric acid method from $[Li^+@C_{60}](PF_6{}^-)$ and characterized its structure by IR, NMR and FAB mass spectroscopy as well as the elemental analysis. Notably, the reaction of $[Li^+@C_{60}](PF_6{}^-)$ was site-selective to give a single major isomer (*ca.* 70%) with two minor isomers in marked contrast to the case of the $Li@C_{60}$ cluster. We concluded from the analysis of radical species produced in the reaction of fuming sulfuric acid and C_{60} cage that this unusual site-selective hydroxylation was caused by the lower HOMO level of lithium encapsulated fullerene than that of empty C_{60}. This result suggests the possibilities of the metal encapsulated fullerenes being capable of becoming a new-type of fullerene multi-adducts with appreciable site-selectivity. Further mechanistic investigation on site-selectivity and the properties of $Li@C_{60}{}^+$ are now undertaken as well as the application of our new Li^+ encapsulated fullerene compounds.

Experimental section

Synthesis of $Li^+@C_{60}O^-(OH)_7$

A slurry of $[Li^+@C_{60}](PF_6{}^-)$ (10 mg, 12 µmol) in 30% fuming sulfuric acid (0.5 mL) was stirred for 48 h at 60 °C under an Ar atmosphere. After cooling to room temperature, the resulting mixture was added dropwise into chilled diethyl ether (100 mL). After centrifugation, the residual solid was washed three times with *ca.* 10 mL of diethyl ether and dried under vacuum at 30 °C. The resulting brown solid was added to water (3 mL) and the mixture was stirred for 48 h at 70 °C in air. After cooling to room temperature, the suspension was filtered and the residual solid was washed with water until the solution was neutralized (40 mL). It was then washed three times with acetonitrile and diethyl ether (40 mL each) and dried under vacuum at 40 °C for 24 h, resulting in $Li^+@C_{60}O^-(OH)_7 \cdot 4H_2O$ (9.2 mg, 9.9 µmol, 83%) as a brown powder.

Acknowledgements

This work was supported by Grant-in-Aid for Exploratory Research (no. 23651111) from JSPS, Japan, and Health Labour Sciences Research Grants from MHLW, Japan. The authors thank Nacalai Tesque Inc. for the helpful guidance of HPLC analysis.

References

1 S. Aoyagi, E. Nishibori, H. Sawa, K. Sugimoto, M. Takata, Y. Miyata, R. Kitaura, H. Shinohara, H. Okada, T. Sakai, Y. Ono, K. Kawachi, K. Yokoo, S. Ono, K. Omote, Y. Kasama, S. Ishikawa, T. Komuro and H. Tobita, *Nat. Chem.*, 2010, **2**, 678–683.

2 (*a*) S. Fukuzumi, K. Ohkubo, Y. Kawashima, D. S. Kim, J. S. Park, A. Jana, V. M. Lynch, D. Kim and J. L. Sessler, *J. Am. Chem. Soc.*, 2011, **133**, 15938–15941; (*b*) K. Ohkubo, Y. Kawashima and S. Fukuzumi, *Chem. Commun.*, 2012, **48**, 4314–4316.